

COVER PAGE

Document downloaded by @DAEL

Sat Nov 28 05:13:34 2026
For personal use

When automatic English translation is provided, only the original document is authentic.
The EAA cannot be held responsible of any translation error

Bibliographical reference

Vibro-Acoustic Modelling of Anisotropic Porous Elastic Materials: A Preliminary Study of the Influence of Anisotropy on the Predicted Performance in a Multi-Layer Arrangement, Peter Göransson and Nils-Erik Hörlin, Acta Acustica **vol. 96** (Number 2), 2010, pp. 258-265

DOI
https://doi.org/10.3813/AAA.918275

ACTA ACUSTICA UNITED WITH ACUSTICA
Vol. 96 (2010) 258 – 265
DOI 10.3813/AAA.918275

Vibro-Acoustic Modelling of Anisotropic Porous Elastic Materials: A Preliminary Study of the Influence of Anisotropy on the Predicted Performance in a Multi-Layer Arrangement

Peter Göransson, Nils-Erik Hörlin
Centre for ECO^2 Vehicle Design & MWL, KTH Aeronautical & Vehicle Engineering, 10044 Stockholm, Sweden. pege@kth.se

Summary
During the recent years considerable efforts have been spent on developing numerical models and performing the necessary characterisation of elastic, dynamic and acoustic properties of porous materials. Originally having been considered to be isotropic, such materials have lately also been studied in terms of their anisotropic properties. In this paper, the influence of anisotropy on the vibroacoustic performance is illustrated and evaluated for a multi-layer configuration with varying boundary conditions between the porous material and a solid plate. The paper starts with a brief review of a recently published anisotropic, mixed displacement pressure weak formulation with a particular emphasis on the anisotropic properties. Using the material properties for a hypothetical porous foam model, the predicted response is evaluated. The influence of anisotropy is found to be significant in terms of response amplitude and apparent damping. For some boundary conditions the predicted response is an order of magnitude lower for the anisotropic material model, in particular for frequency ranges where the dynamics of the foam are significant.

PACS no. 43.20.-f, 43.40.-r

1. Introduction

In many applications, the assumption of isotropic porous material properties allows for satisfactory correlations between experimental and computed results. However, in more complex configurations the sometimes rather poor agreement is at present an issue of extensive discussion. In particular, for porous models in the scope of classical vibroacoustics applications and specifically these where the structure borne properties are important, the sources of differences in predicted and measured results are not fully understood. There are several plausible explanations for such deviations, e.g., the modeling of coupling conditions between components, spatial variation in properties, etc. which all may affect the behavior of the system. However, in order to assess the possible influence of anisotropy on the vibroacoustic behaviour, extensive and detailed studies are necessary as a basis for motivation of the need for this quite complicated material modelling. Nevertheless, whereas the anisotropic feature of real porous materials, may pose complications in terms of the complex characterisation of the parameters representing an actual material, it does however also bring a potential for tailoring and design of the vibro-acoustic properties to reach an overall benefit in terms of control of unwanted vibrations and acoustic phenomena.

Results from predictions using weak formulations and associated finite element solutions to the equations modelling anisotropic porous media, have up to now not been discussed to any greater extent in the acoustic literature. The present paper uses such a weak formulation of Biot's original equations based on a mixed displacement-pressure formulation with general anisotropy. Finite element solutions are obtained for several multi-layer configurations, varying the coupling conditions between the components. Three cases are studied, all using as a common baseline, a porous material bonded to an elastic plate. The opposite surface of the porous material is either free, coupled to a plate in elastic contact (bonded) or coupled to a plate through a finite layer of air (unbonded). The results for a hypothetical porous material are compared to results obtained using an equivalent isotropic material model of the involved porous components.

2. Related work

Biot initially discussed the equations governing the behaviour of an anisotropic poro-elastic medium in [1], [2] and [3]. However, most of the published work discussing prediction models, based on finite element modelling of Biot's equations, have with a few exceptions been limited

Received 23 June 2009,
accepted 15 January 2010.

© S. Hirzel Verlag · EAA

to isotropic material descriptions. One such example is the perhaps most commonly used formulation based on mixed displacement-pressure variables [4], which was formulated for isotropic materials. Gorog *et al.* discussed anisotropic weak formulations using the displacements as dependent variables and outlined a formulation for a mixed variable solution [5]. However, no results for an anisotropic material model were discussed. Rice *et al.* discussed a transversely isotropic finite element solution using a mixed displacement-pressure potential formulation and applied it to a fibrous wool [6]. Predicted vibration transmissibility results correlated very well with experiments for two different glass fibre wool materials in a seismic mass configuration.

Studies of multilayer configurations, with finite lateral dimensions, have been published lately, see e.g. [7], [8]. In the latter paper the influence of boundary conditions between different, isotropic, layers were discussed in terms of transmission into a finite sized cavity. Simulations based on transfer matrix modelling of transversely isotropic materials has recently been studied by Khurana *et al.* [9].

Experimental investigations focusing on the effects of anisotropy have also been discussed lately. Allard *et al.* studied the effect of anisotropy on the normal impedance for glass wool [10]. In the investigations performed by Rice *et al.* [11] the influence of an adjacent porous foam separated by a varying airgap on the damping of a vibrating plate was discussed. The results indicated quite strong variations of the damping with the airgap thickness. Similarly anisotropic mineral and glass wool models have been investigated, confirming the high degree of anisotropy for elasticity, see [12], and for flow resistivity, see [13].

3. Governing equations

Following Biot and Willis [1] and a transformation to mixed displacement pressure dependent variables, a fully anisotropic formulation is presented. The mixed anisotropic formulation is an analogue of the weak statement derived by Atalla *et al.* [4], assuming that the material constituting the solid frame is linearly elastic and isotropic. This is a reasonable approximation, implying that the anisotropy of the porous material is entirely related to the geometry of the microstructure.

The notations used are explained throughout the paper, but some recurring uses are that boldface indicates tensors, superscripts are used to identify: quantities related to zero acoustic pressure conditions, 0; quantities related to unjacketed conditions, u; variables associated with the solid frame, s; variables associated with the fluid in the pores, f; and subscripts are used to identify: quantities projected on normal to surface, n; component ordinal numbers in Cartesian co-ordinate system, e.g. $i = 1, 2, 3$ as i, j, k; partial derivative with respect to Cartesian co-ordinate x_i as $(.)_{,i} = \partial(.)/\partial x_i$. Displacements are identified as u_i^f for the fluid displacement, u_i^s for the solid frame displacement and p is used for the acoustic pore pressure. The porosity, i.e. open volume to total volume of porous material is ϕ and Kronecker's delta is δ_{ij}. In the following also Cartesian tensor notation with Einstein's summation convention, i.e., repeated indices imply a summation of these terms, is used unless otherwise noted. Finally ω is used for the angular frequency in [radians/s].

3.1. Anisotropic displacement pressure formulation

The complete derivation of the anisotropic displacement pressure formulation is beyond the scope of the present paper, focusing on the influence of anisotropy itself rather than its modelling. Thus, as a starting point for the discussion, the anisotropic mixed variable equations recently proposed by the authors, [14], are here summarised as

$$\begin{aligned} -C_{ijkl}u^s_{k,l} - \phi\left(\delta_{ij} + \frac{Q_{ij}}{R}\right)p \\ -\omega^2\left(\tilde{\rho}^{11}_{ij} - \tilde{\rho}^{12}_{ik}\hat{\rho}^{22}_{kl}\tilde{\rho}^{12}_{lj}\right)u^s_j \\ -\phi\left(\delta_{ij} + \tilde{\rho}^{12}_{ik}\hat{\rho}^{22}_{kj}\right)p_{,j} = 0, \end{aligned} \tag{1}$$

$$\begin{aligned} -\frac{\phi^2}{R}p - \phi\left(\delta_{kl} + \frac{Q_{kl}}{R}\right)u^s_{k,l} - \frac{\phi^2}{\omega^2}\hat{\rho}^{22}_{kj}p_{,kj} \\ +\phi\left(\delta_{jl} + \hat{\rho}^{22}_{kj}\tilde{\rho}^{12}_{kl}\right)u^s_{l,j} = 0, \end{aligned} \tag{2}$$

where $\hat{C}_{ijkl}$ is the solid frame Hooke's matrix,

$$R = \frac{\phi^2 K_s}{1 - \phi - K_s C_{ijkl} d_{ij} d_{kl} + \phi K_s / K_f}, \tag{3}$$

$$Q_{ij} = \frac{\left[(1-\phi)\,\delta_{ij} - C_{ijkl}d_{kl}\right]\phi K_s}{1 - \phi - K_s C_{ijkl} d_{ij} d_{kl} + \phi K_s / K_f}, \tag{4}$$

and K_s is the unjacketed frame compressional modulus, d_{ij} the unjacketed compressibility compliance tensor, further discussed below.

Note that in the present model of an anisotropic porous material, the fluid itself is assumed to be isotropic and hence R is a scalar quantity, in which the fluid compressibility, K_f is obtained using the model by Lafarge *et al.*, [15]. However, due to the assumed elastic anisotropy of the solid phase, the dilatational coupling parameter Q_{ij} is a second order tensor.

Similarly, the equivalent density tensors, $\tilde{\rho}^{11}_{ij}$, $\tilde{\rho}^{12}_{ij}$ *and* $\tilde{\rho}^{22}_{ij}$, and the tortuosity tensor, α_{ij}, are anisotropic generalisations of the equivalent densities used e.g. by Allard [16], and may be defined as

$$\tilde{\rho}^{11}_{ij} = \rho_1\delta_{ij} + \rho^a_{ij} - \frac{\mathrm{i}}{\omega}b_{ij}, \tag{5}$$

$$\tilde{\rho}^{12}_{ij} = \rho^a_{ij} + \frac{\mathrm{i}}{\omega}b_{ij}, \tag{6}$$

$$\tilde{\rho}^{22}_{ij} = \phi\rho_0\delta_{ij} + \rho^a_{ij} - \frac{\mathrm{i}}{\omega}b_{ij}, \tag{7}$$

$$\rho^a_{ij} = \left(\alpha_{ij} - \delta_{ij}\right)\phi\rho_0 \tag{8}$$

with ρ_0 as the ambient fluid density, ρ_1 as the bulk density of the porous material.

$$\hat{\rho}^{22}_{ik}\tilde{\rho}^{22}_{kj} = \delta_{ij}, \tag{9}$$

i.e., $\hat{\rho}^{22}_{ik}$ is the inverse of $\tilde{\rho}^{22}_{jk}$, assuming that the viscous drag tensor, b_{ij}, is invertible, [17], [18].

The reasons for the complex densities being written as second order tensors, are due to the presence of two terms, b_{ij}, the viscous drag tensor and the tortuosity tensor α_{ij}. These may, following traditional modelling of porous materials, either be calculated from the static flow resistivity tensor $\sigma_{ij}^{\text{flow}}$, see e.g. [18], or for the tortuosity tensor, α_{ij}, be deduced from simulations or measurements on anisotropic porous micro-structural, geometries, e.g., through potential fluid flow considerations.

3.2. Anisotropic mixed weak formulation

To obtain the weak form, equation (1) was multiplied by a test function v_i^s, and the resulting expression integrated over the domain, Ω, e.g. in the finite element method this would be the domain of an element, and after application of Gauss theorem, the solid frame equation was obtained as

$$\begin{aligned}
&\int_\Omega \left[C_{ijkl} u^s_{k,l} - \phi \left(\delta_{ij} + \frac{Q_{ij}}{R} \right) p \right] v^s_{i,j} \, \mathrm{d}\Omega \\
&+ \int_\Omega \Bigg[- \omega^2 \left(\tilde{\rho}^{11}_{ij} - \tilde{\rho}^{12}_{ik} \hat{\rho}^{22}_{km} \tilde{\rho}^{12}_{mj} \right) u^s_j \\
&- \phi \left(\delta_{ij} + \tilde{\rho}^{12}_{ik} \hat{\rho}^{22}_{kj} \right) p_{,j} \Bigg] v^s_i \, \mathrm{d}\Omega = \int_\Gamma T^{\text{tot}}_i v^s_i \, \mathrm{d}\Gamma,
\end{aligned} \tag{10}$$

where the total traction vector is $T_i^{\text{tot}} = \sigma_{ij}^{\text{tot}} n_j$ along the boundary Γ.

Similarly, multiplication of equation (2) by a test function q and integration over the domain, followed by application of Gauss theorem to the two last terms, the fluid phase equation was obtained as

$$\begin{aligned}
&\int_\Omega \left[-\phi \left(\delta_{kl} + \frac{Q_{kl}}{R} \right) u^s_{k,l} - \frac{\phi^2}{R} p \right] q \, \mathrm{d}\Omega \\
&+ \int_\Omega \Bigg[- \phi \left(\delta_{jm} + \hat{\rho}^{22}_{jk} \tilde{\rho}^{12}_{km} \right) u^s_m \\
&+ \frac{\phi^2}{\omega^2} \hat{\rho}^{22}_{jk} p_{,k} \Bigg] q_{,j} \, \mathrm{d}\Omega = \int_\Gamma \phi u^{\text{rel}}_{\mathbf{n}} q \, \mathrm{d}\Gamma,
\end{aligned} \tag{11}$$

where u_i^{rel} is the relative displacement between solid frame and pore fluid.

Equations (10) and (11) together constitute a symmetric weak representation of the anisotropic Biot equations in terms of the frame displacement vector u_i^s and the fluid pore pressure p, which for the analyses discussed in the present work has been implemented in the in-house hierarchical finite element code developed by the authors [19] [20].

4. Simulation of anisotropic foam plate combinations

To investigate the effects of anisotropy in the foam properties, a series of numerical experiments were designed in the form of three different quadratic plate-foam combinations and as a basis for discussion the bare steel plate itself. The foam was then modelled either as an anisotropic or as an isotropic material, and the predicted response evaluated for different multi-layer arrangements. Three different configurations have been investigated in this work, see Table I, the variations being whether or not a top plate was present, and if it was included, the corresponding attachment conditions. For the predictions, the numerical simulations were made over a range of frequencies, using the mesh shown in Figure 1 and constant polynomial order of the shape functions used in the hierarchical finite elements.

Table I. Configurations studied

Case	Combination	Thickness
1	Steel plate	0.001 m
"	Foam	0.042 m
2	Steel plate	0.001 m
"	Foam	0.042 m
"	Steel plate	0.001 m
3	Steel plate	0.001 m
"	Foam	0.042 m
"	Air gap	0.001 m
"	Steel plate	0.001 m

The isotropic foam material model was derived as an equivalent of the anisotropic ditto, in the sense that the anisotropic foam was elastically compressed in the z-direction, i.e., in the same direction as the load was applied in the simulations performed, see Figure 1. A unit, static load was used in the numerical model and the corresponding Young's modulus computed from the resulting deformation. Admittedly, this is to a large extent an arbitrary equivalency, which by no means was intended to be accurately describing the actual foam in an isotropic model. However, for the purpose of illustrating the effects of anisotropy it should fulfil its purpose, an assumption supported by the relatively close agreement at low frequencies, indicating that the static modulus thus calculated is reasonable, see section 5.

The general geometry of the test problem is shown in Figure 1 and the three different plate foam combinations studied are shown in Table I. For the case where the top plate was not in contact with the foam, case 3, an airgap was included in order to separate foam and cover plate, see Figure 2. In all cases, the foam was bonded to the lower steel plate. The excitation was applied as a unit amplitude, uniform traction over one element at the solid plate surface, see Figure 1. This choice of excitation is based on an interest in the influence of the anisotropy of the foam for the particular case of structure-borne excitation, where the effects could be expected to be significant due to the strong elastic anisotropy of the hypothetical foam studied here. The model has homogenous natural boundary conditions along all free surfaces, except the excited element surface. For a solid plate, this implies traction free bound-

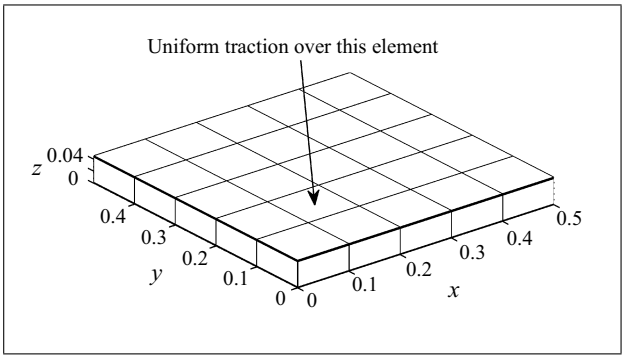


Figure 1. Model problem used in simulation of anisotropic foam formulation. $L_x = 0.5$m , $L_y = 0.5$m, foam thickness 0.0425m and steel plate thickness 0.001m. Note that the excitation is applied at the opposite (hidden) side of the mesh shown.

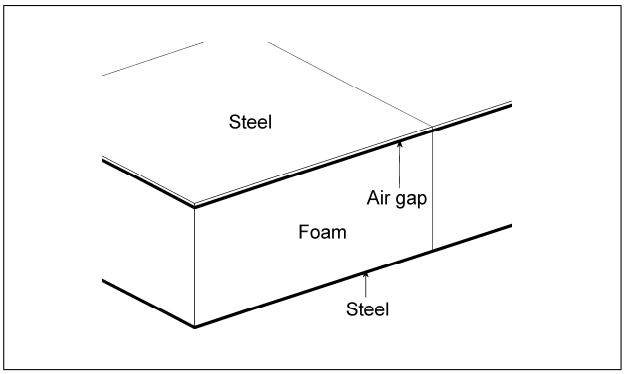


Figure 2. Detail of model for unbonded steel plate problem, case 3, used in study of effects of anisotropic foam. Airgap thickness 0.001 m.

Table II. Common parameters used in the foam models.

Material parameter	Value	Unit
Frame bulk density	22.1	kg/m^3
Frame loss factor	0.0	
Porosity	0.98	
Fluid density	1.204	kg/m^3
Fluid dynamic viscosity	$1.84 \cdot 10^{-5}$	Ns/m^2
Fluid ratio of specific heats	1.4	
Prandtl number	0.71	
Viscous characteristic length	$1.1 \cdot 10^{-4}$	m
Thermal characteristic length	$7.4 \cdot 10^{-4}$	m
Thermal form factor	0.25	
Gas constant (for air)	286.7	$m^2/(s^2K)$
Absolute temperature	293.15	K

aries. For the porous material modelling using a mixed displacement-pressure formulation, homogeneous natural boundary conditions amount to traction free boundaries, see right hand side of equation (10), and zero relative displacement, see right hand side of equation (11).

The material parameters used that were common to both material models are shown in Table II, and the specific parameters used for the isotropic equivalent model are shown in Table III and for the anisotropic model in equations (13), (14) and (15). Note that some of the parameters have been taken from known, previously characterised foams but the actual composition used here is hypothetical, i.e. this foam does not necessarily exist.

Table III. Parameters specific to the isotropic foam material model.

Material parameter	Value	Unit
Frame Young's modulus	$100.0 \cdot 10^3$	Pa
Frame Poisson's ratio	0.4	
Static flow resistivity	60000	kg/m^3s
Tortuosity	1.3	

The structural damping related to the solid frame of the porous material, has been assumed to be zero in the current simulations, both for the anisotropic material as well as for the isotropic equivalent. There were two main reasons for this restriction of the model, one phenomenological and one more fundamental. Starting with the latter aspect, the modelling of damping for an anisotropic porous materials is as yet an open issue. In its essence, this comes down to the question whether the dissipation mechanisms follow the same directional dependencies as the elastic moduli or they have their own material co-ordinate system? In [6] the damping for the solid frame was assumed to be following an isotropic material law, while the elastic moduli were taken to be transversely isotropic. However, recent results, see [21], suggest that these dissipation mechanisms have their own directional dependencies. Thus, in order to avoid a confusing discussion on the effect of the assumed damping modelling, and at the same time allow for a focused study of the effects of the anisotropoic flow resisitivity which is the major source of losses in the studied models, the structural losses were omitted.

Frequency spectra between 1 and 500 Hz with 1 Hz resolution were calculated using hierarchical polynomials of order 4, for the two different material models. In order to study the influence of anisotropy more closely, the vibration response of the upper non-excited surface, in the 3-direction normal to the surface, was evaluated. This means for the porous material on steel plate, case 1, the vibration of the solid frame of the foam and for the two cases where another solid plate was introduced, case 2 and case 3, the vibration of the plate. The purpose was to illustrate the transmission of both acoustic pressure and vibration response through the multi-layered configuration, when the foam is modelled as either anisotropic or as an equivalent isotropic ditto.

$$W_\Gamma^2(\omega) = \int_\Gamma u_3(\omega)\,\bar{u}_3(\omega)\,\mathrm{d}\Gamma. \tag{12}$$

$$\boldsymbol{\sigma}^{flow} = \begin{bmatrix} 37\,500 & 0 & 0 \\ 0 & 37\,500 & 0 \\ 0 & 0 & 67\,500 \end{bmatrix} [\mathrm{Pa\,s/m^2}], \tag{13}$$

$$\boldsymbol{\alpha} = \begin{bmatrix} 1.2 & 0 & 0 \\ 0 & 1.2 & 0 \\ 0 & 0 & 1.5 \end{bmatrix}, \tag{14}$$

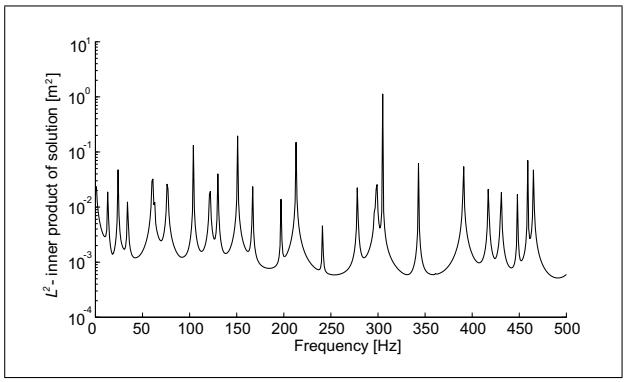


Figure 3. Response of steel plate, calculated using equation (12).

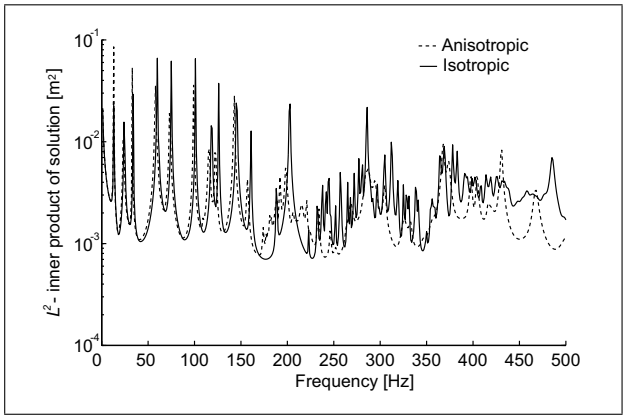


Figure 4. Response of upper foam surface, case 1, spectra calculated using anisotropic and isotropic material data according to equation (12).

$$\mathbf{C} = \begin{bmatrix} 40 & 33 & 37 & 0 & 0 & 0 \\ & 89 & 131 & 0 & 0 & 0 \\ & & 300 & 0 & 0 & 0 \\ & & & 26 & 0 & 0 \\ symm. & & & & 21 & 0 \\ & & & & & 26 \end{bmatrix} \cdot 10^3 [\text{Pa}]. \qquad (15)$$

The influence of the directional dependence of the material properties may further be illustrated by computing the transmissibility, here defined as the ratio of the summed squares of the normal displacement of the upper plate, using equation (12), to the same quantity calculated for the excited plate. This quantity was calculated for all three cases studied and are discussed below.

5. Discussion

For all cases, the resonances of the steel plate itself, see Figure 3, are dominating the response up to about 175 Hz. Above that frequency the resonances of the foam become noticeable, in particular for the two cases with a free upper surface of the foam. For case 2, some interaction frequencies may be detected above 250 Hz, which is also the frequency above which the two prediction models for the foam start to deviate from each other, even though for this particular case the deviation is rather small. From Figure 5,

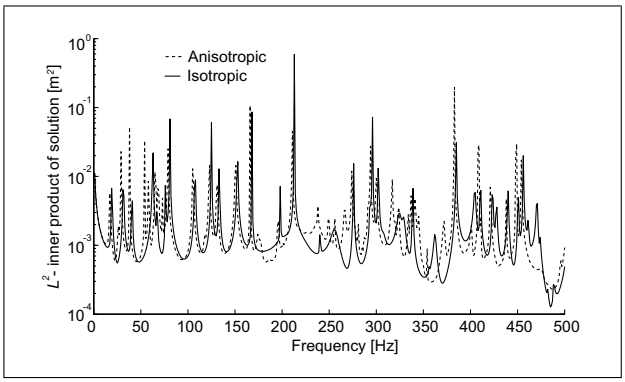


Figure 5. Response of upper bonded steel plate, case 2, spectra calculated using anisotropic and isotropic material data according to equation (12).

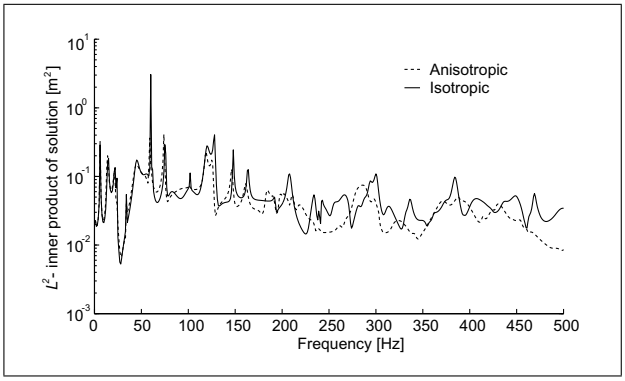


Figure 6. Response of upper steel plate, case 3, spectra calculated using anisotropic and isotropic material data according to equation (12).

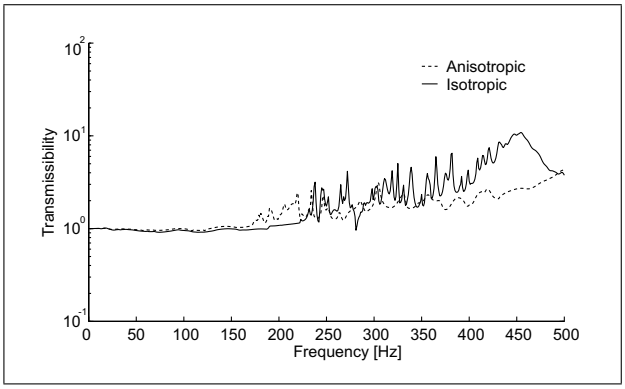


Figure 7. Ratio between responses, evaluated according to equation (12), of upper foam surface and excited (lower) plate, case 1, calculated using anisotropic and isotropic material data.

it may also be seen that the anisotropic model predict resonance peaks that are not captured by the isotropic model and vice versa. The latter may also be observed in the other two cases, Figure 4 and Figure 6, and is perhaps most emphasised in case 3 where few peaks above 175 Hz appear at the same frequencies in the comparison of the two models.

An interesting result of the analysis results obtained using the two different material models for the foam, is that for Cases 1 and 3 the apparent damping is considerably

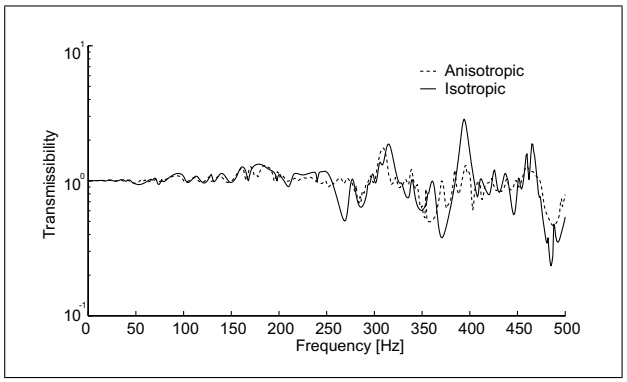


Figure 8. Ratio between responses, evaluated according to equation (12), of upper plate and excited (lower) plate, case 2, calculated using anisotropic and isotropic material data.

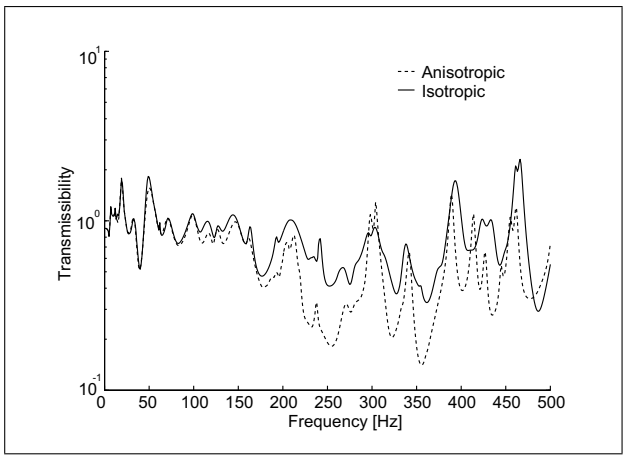


Figure 9. Ratio between responses, evaluated according to equation (12), of upper plate and excited (lower) plate, case 3, calculated using anisotropic and isotropic material data.

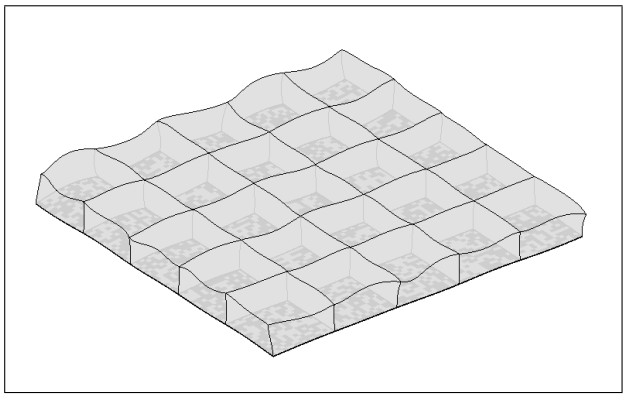


Figure 10. Real part of displacement at 400 Hz for case 1, using anisotropic modelling of foam. Magnification factor $5 \cdot 10^4$.

higher for the anisotropic material model, for frequencies above 175 Hz, as compared to the isotropic ditto. This suggests that the unrestrained motion of the upper surface is differently predicted and is influencing the foam behaviour substantially, giving rise to higher in-plane deformations and corresponding relative motion in the anisotropic model. Evidence supporting this, may be seen in

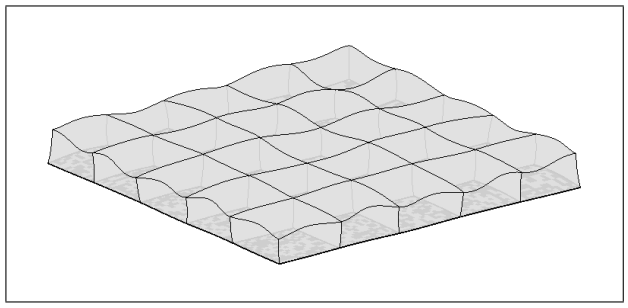


Figure 11. Real part of displacement at 400 Hz for case 1, using isotropic modelling of foam. Magnification factor $5 \cdot 10^4$.

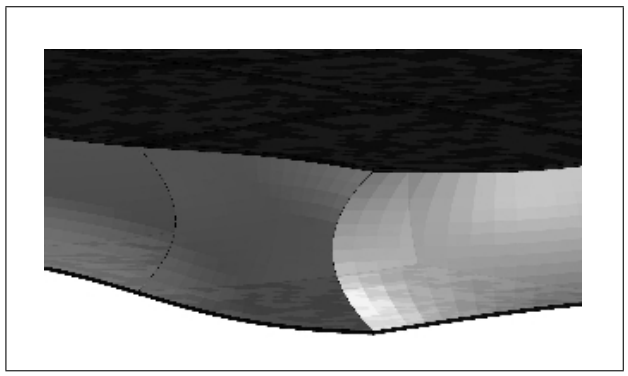


Figure 12. Real part of displacement at 400 Hz for case 2, using anisotropic modelling of foam. Magnification factor $5 \cdot 10^4$.

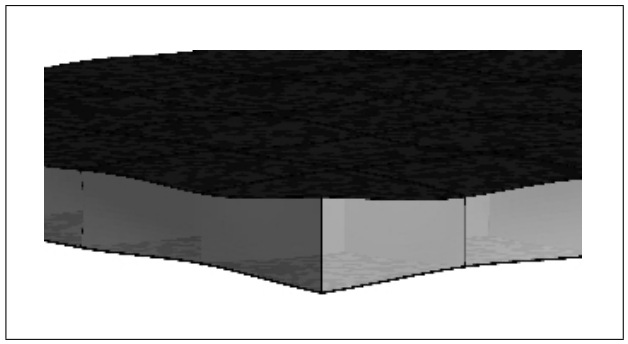


Figure 13. Real part of displacement at 400 Hz for case 2, using isotropic modelling of foam. Magnification factor $5 \cdot 10^4$.

Figures 10 and 11 for case 1 and in Figures 14 and 15 for case 3. The increased deformation in the transverse direction which may be seen in these figures, contributes to the increase in observed damping, recalling that the losses in the solid frame part of the porous material, was neglected in the current simulations. The fact that the influence of anisotropy is particularly evident in the cases where the upper foam surface is free, is interesting since it could be expected that the role of the structure borne path is less important, and hence also the influence of the assumed anisotropy which is strongest in the elastic part. However, in the configurations and for the material studied here this seems not be the case, partially due to the high flow resistivity and tortuosity assumed, coupling the elastic and fluid strongly together.

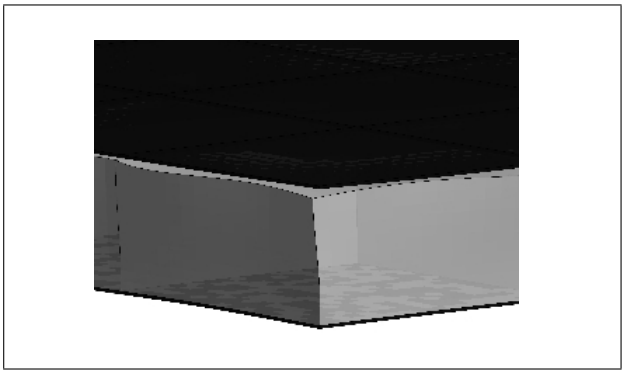


Figure 14. Close up of real part of displacement at 400 Hz for case 3, using anisotropic modelling of foam. Magnification factor $3 \cdot 10^4$.

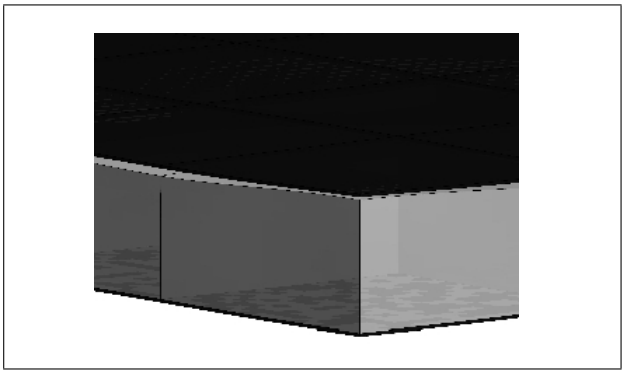


Figure 15. Close up of real part of displacement at 400 Hz for case 3, using isotropic modelling of foam. Magnification factor $3 \cdot 10^4$.

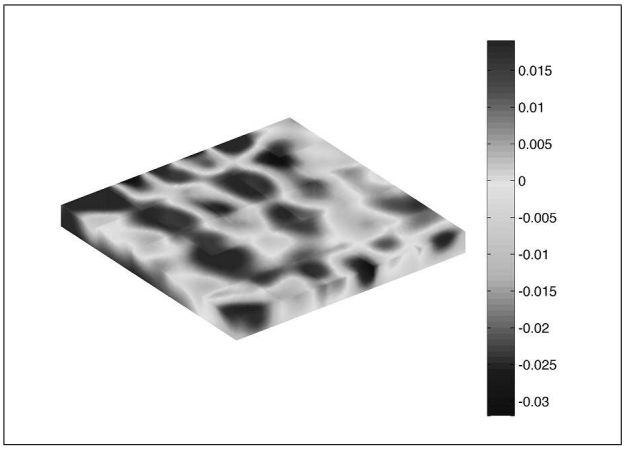


Figure 16. Real part of acoustic pressure in foam at 400 Hz for case 1, using anisotropic modelling of foam. Scale in [Pa].

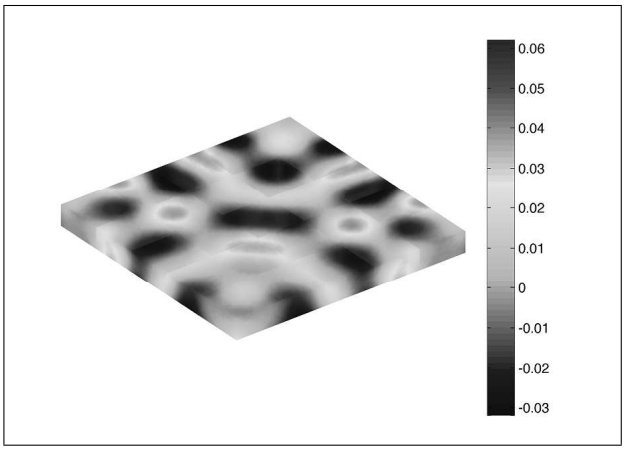


Figure 17. Real part of acoustic pressure in foam at 400 Hz for case 1, using isotropic modelling of foam. Scale in [Pa].

For the bonded configuration, case 2, the in-plane deformation is also higher in the anisotropic results, compare Figures 12 and 13, but due to the restraining solid plate boundaries the amplitudes are limited and hence also the increase in damping.

For the foam-plate combination with a free upper surface of the porous material, case 1, the assumption of an isotropic material appears to be conservative in terms of response levels over most of the frequency range investigated, see Figure 4. This actually holds also for case 3, with the airgap separating the porous layer and the solid plate, see Figure 6. For case 2, where the porous layer is bonded to both plates, the effect of anisotropy is marginal for the material properties studied here, see Figure 5, and where significant the tendency is that the isotropic model is non-conservative.

To further illustrate the differences between an anisotropic foam and its isotropic equivalent, Figures 16 and 17 show for case 1 the acoustic pressure variation in the foam. The shorter wave lengths in the anisotropic pressure map, reflect the higher degree of transverse motion discussed above.

In addition to the responses evaluated and discussed above, the transmissibility was computed using the responses from the two material models. In agreement with the observed dominance of the steel plate resonances, the transmissibility is well predicted by the isotropic foam model up to about 175 Hz for case 1 and 2 but slightly worse for case 3, where the free upper surface of the foam allows for transverse effects, see Figures 7, 8 and 9. The predicted ratio is close for anisotropic and isotropic modelling of the porous layer in case 2, whereas for case 3 it differs substantially. However, also for this evaluated quantity, the apparent system damping predicted with the isotropic model is lower. In general, the influence of the anisotropic modelling of the foam, is important in the frequency range where the foam dynamics becomes noticeable, i.e. above about 175 Hz for all three cases studied. The amplitude differences in the computed transmissibility are quite significant for higher frequencies. For Case 1, with the free foam surface and no upper plate, the difference may be up to a factor of 4 over certain frequency, see Figure 7, and for case 3 where the foam upper surface is unrestrained but has a plate close to it, see Figure 9, the difference is about a factor 3 over about 225 Hz. For case 2, the influence of anisotropy is more complex, see Figure 8. Similar to the other two cases, the apparent damping is higher for the anisotropic model, but the influence is less for certain peaks in the transmissibility curve while it is

quite significant for some, with magnitude differences up to a factor of 3. This frequency ranges, appear to be related to differences in the predicted coupled behaviour of the two plates with the foam bonded to both.

6. Concluding remarks

The results discussed in this paper suggest that the influence of anisotropy is important as soon as the foam starts to interact strongly with, in this paper, a vibrating plate. This was a more or less expected outcome of the current investigation and the rather simplified anisotropy chosen. A more interesting result perhaps is the observation made concerning the apparent damping, that may be inferred from the response curves. Keeping in mind that the only losses included are related to the viscous and thermal interactions, this must then be related to the relative motion between solid frame and fluid in the porous material being more pronounced for the anisotropic model. This is an interesting result, in particular in view of the higher flow resistivity used for the transverse directions in the isotropic model. Evaluation of the transverse displacements and pressure distributions inside the foam, tending to have shorter wavelengths in the anisotropic material model, support this preliminary conclusion.

As a final comment, it should be noted that the current material models are hypothetical and lack in several aspects. For example are all material tensors written in their principal form, assuming that they all share the same material co-ordinate systems and that these are aligned with the body co-ordinate system of the simulated configuration. In a real material, this is not to be expected and furthermore, if different material systems would be present, coupling between different deformations could change the results completely. To generalise the results from the present preliminary study, is difficult as a more realistic material would exhibit more complex interaction. Hence, a similar analysis should be conducted for a real material, i.e. with material properties based on characterisation of a foam or fibrous wool.

References

[1] M. A. Biot, D. G. Willis: The elastic coefficients of the theory of consolidation. Journal of Applied Mechanics **24** (1957) 594–601.

[2] M. A. Biot: Mechanics of deformation and acoustic propagation in porous media. Journal of Applied Physics **33** (1962) 1482–1498.

[3] M. A. Biot: Generalized theory of acoustic propagation in porous media. The Journal of the Acoustical Society of America **34** (1962) 1254–1262.

[4] N. Atalla, M. A. Hamdi, R. Panneton: Enhanced weak integral formulation of the mixed (u,p) poroelastic equations. The Journal of the Acoustical Society of America **109** (2001) 3065–3068.

[5] S. Gorog, R. Panneton, N. Atalla: Mixed displacement-pressure formulation for acoustic anisotropic open porous media. Journal of Applied Physics **82** (1997) 4192–4196.

[6] H. Rice, P. Goransson: A dynamical model of light fibrous materials. International Journal of Mechanical Science **41** (1999) 561–579.

[7] P. Göransson: Acoustic and vibrational damping in porous solids. Philosophical Transactions of the Royal Society. Series A **364** (2006) 89–108.

[8] P. Göransson: Tailored acoustic and vibrational damping in porous solids. Engineering performance in aerospace applications. Aerospace Science and Technology **364** (2006) 89–108.

[9] P. Khurana, L. Boeckx, W. Lauriks, P. Leclaire, O. Dazel, J. F. Allard: A description of transversely isotropic sound absorbing materials by transfer matrices. The Journal of the Acoustical Society of America **125** (2009) 915–921.

[10] J. F. Allard, R. Bourdier, L'Esperance: Anisotropic effect in glass wool on normal impedance in oblique incidence. Journal of Sound and Vibration **114** (1987) 233–238.

[11] H. J. Rice, A. Cumings, R. Wilson: Radiation damping in plates, induced by porous media. Journal of Sound and Vibration **221** (1999) 143–167.

[12] J. Tran-Van, X. Olny: Acoustic and elastic parameters determination for anisotropic mineral wools. Acta Acustica united with Acustica **91** (2005) S20.

[13] V. Tarnow: Measured anisotropic air flow resistivity and sound attenuation of glass wool. The Journal of the Acoustical Society of America **12** (2008) 26–41.

[14] N.-E. Hörlin, P. Göransson: Weak, anisotropic symmetric formulations of Biot's equations for vibro-acoustic modelling of porous elastic materials. International Journal of Numerical methods in Engineering (2010) submitted.

[15] D. Lafarge, P. Lemarinier, J. F. Allard, V. Tarnow: Dynamic compressibility of air in porous structures at audible frequencies. The Journal of the Acoustical Society of America **102** (1997) 1995–2006.

[16] J. F. Allard: Propagation of sound in porous media: Modelling sound absorbing materials. Elsevier Applied Science, ISBN 0-387-98319-8.

[17] L. Wang: Flows through porous media: A theoretical development at macroscale. Transport in Porous Media **39** (2000) 1–24.

[18] P. Göransson, R. Guastavino, N.-E. Hörlin: Measurement and inverse estimation of 3d anisotropic flow resistivity for porous materials. Journal of Sound and Vibration **327** (2009) 354–367.

[19] N.-E. Hörlin, M. Nordström, P. Göransson: A 3d hierarchical fe formulation of Biot's equations for elasto-acoustic modelling of porous media. Journal of Sound and Vibration **245** (2001) 633–652.

[20] N.-E. Hörlin: 3D hierarchical hp-FEM applied to elasto-acoustic modelling of layered porous media. Journal of Sound and Vibration **285** (2005) 341–363.

[21] R. Guastavino, P. Göransson: Modeling and characterisation of the vibration dynamics modeling of anisotropic porous foam materials. Proceedings of ISMA2006: International Conference on Noise and Vibration Engineering, 2006, 1481–1487.